Fermilab Proposal No. 391

Scientific Spokesman:

M. Strovink
Lawrence Berkeley Laboratory
Berkeley, California 94720

FTS/Com: 415 - 843-2740
Ext. 5501

EXPLORATION OF RARE MUON-INDUCED PROCESSES

(ADDENDUM II TO FERMILAB PROPOSAL 203)

A. R. Clark, E. S. Groves, L. T. Kerth,
S. C. Loken, M. Strovink, W. A. Wenzel

Department of Physics and
Lawrence Berkeley Laboratory,
University of California, Berkeley, CA 94720

and

R. Cester, F.C. Shoemaker, P. Surko, M.S. Witherell

Joseph Henry Laboratories,
Princeton University, Princeton, N. J. 08540

and

R. P. Johnson
Fermi National Accelerator Laboratory
Batavia, Ill. 60510

February 18, 1975

Correspondent: M. Strovink
FTS/COM 415-843-2740 Ext. 5501

EXPLORATION OF RARE MUON-INDUCED PROCESSES

(ADDENDUM II TO FERMILAB PROPOSAL 203)

A. R. Clark, E. S. Groves, L. T. Kerth,
S. C. Loken, M. Strovink, W. A. Wenzel

Department of Physics and
Lawrence Berkeley Laboratory,
University of California, Berkeley, CA 94720

and

R. Cester, F.C. Shoemaker, P. Surko, M.S. Witherell

Joseph Henry Laboratories,
Princeton University, Princeton, N. J. 08540

and

R. P. Johnson
Fermi National Accelerator Laboratory
Batavia, Ill. 60510

February 18, 1975

I. INTRODUCTION

Now that the Fermilab muon beam has exceeded design intensity and provided significant illuminations to both first-stage muon scattering experiments, the program requires experimental apparatus which would realize a broader range of muon physics objectives. High acceptance over the full length of a distributed iron target-spectrometer can provide the necessary sensitivity to rare processes. Nearly continuous iron can suppress $\pi \to \mu\nu$ decay background and provide the medium for calorimetric determination of energy transfer to hadrons. Fast detectors can tolerate further increases in beam intensity while maintaining acceptance for multiple final-state muons even within the beam area.

We first proposed to build such a spectrometer two years ago. The purpose of this Addendum is to consolidate the experimental groups who would participate in the experiment, to present further information on its design and implementation, and to update our physics objectives. In addition, we describe the capabilities of the experiment which have direct relevance to recent discoveries of new particles[1] and evidence of direct muon production[2]. The first two topics are addressed in section II and the Appendices; the initial experimental objectives are enumerated below and described in greater detail in part III. Longer-range plans are described in part IV.

The initial physics objectives are mutually compatible. They are:

(1) Search for heavy neutral muons predicted by gauge theories in the mass range 2 - 10 GeV, and other new particles decaying into one muon. The sensitivity for analyzed events is $1 - 2 \times 10^9$ events/μb.

(2) Measurement of deep-inelastic virtual Compton scattering and search for other deep-inelastic $\mu^+\mu^-$ pair creation.

(3) Measurement of the deep-inelastic muon scattering structure function at very high momentum transfers. For example, 8200 events exceeding $Q^2 = 160$ $(GeV/c)^2$ will be obtained.

(4) Collection of $2 - 3 \times 10^4$ $\psi \rightarrow \mu^+\mu^-$ decays and data at higher dimuon masses. The $\psi\mu\mu$ coupling will be measured in the range -15 $(GeV/c)^2 < q^2 < 0$ with 7% statistics at $q^2 = -m_\psi^2$.

II. THE SPECTROMETER

The design of the magnetized iron spectrometer, shown in Figure 1, is substantially the same as that described in the original proposal. We will discuss here only those features which have changed.

The total length of iron in the spectrometer has been decreased from 50 ft to 30 ft, and the cross-section of the active area has been increased to 3.5 x 6 ft (from 3 x 4 ft). These changes reduce the tonnage of iron by 31% from the original proposal. Compensating improvements in acceptance and in detector information will minimize the effect of this change on the yield of events passing final cuts. The decreased length makes possible a finer granularity in the detector system, giving more and higher quality information for each event.

The details of one module of the spectrometer are shown in Figure 2. The apparatus consists of 18 such units. Each module consists of 5 magnetized iron plates, 4 inches thick. Between each plate is a calorimeter counter similar to those described in Proposal 307, Appendix C. These provide a measurement of the hadron energy with accuracy $\sigma(E) \approx 0.9\,E^{\frac{1}{2}}$. In addition, the calorimeter counters locate the interaction vertex for "noisy" events and are used in the trigger logic to detect showers and to veto unscattered muons. Three independent triggers, using the same counter hodoscopes, will be used in parallel. A thorough discussion of trigger efficiencies and rates appears in Appendix 4.

At the downstream end of each module there is a fifth calorimeter counter and a proportional counter-drift chamber system to locate precisely secondary muon tracks as well as the incident track upstream of the interaction. Alternate banks also contain a trigger hodoscope for the single and multiple muon triggers. An exploded view of the trigger-detector system is shown in Figure 3.

The use of proportional chambers, as originally proposed, provides the good time resolution and multitrack efficiency necessary to take data at instantaneous beam fluxes up to 10^7/ sec. We have added a drift chamber to each detector to achieve high spatial resolution in the bending plane. This results in a significant improvement in momentum resolution, which ranges from 7% to 11%.

The engineering group at LBL has made an independent conservative cost estimate of the muon spectrometer. This study (Appendix 1) indicates that the total cost of the magnet will be less than $240 K. The cost of instrumentation (Appendix 2) is less than $210 K.

The time scale for construction, assuming approval is received at the March meeting of the PAC, is shown in Fig. 5. Installation of the spectrometer can begin in February 1976. The critical path is determined by the delivery time for the steel. An informal quote from a supplier is 5 months. If distressed steel is available, the time scale can be accelerated by several months.

As indicated in Appendix 3, the responsibility for the construction and installation of the apparatus will be shared by all of the collaborators. There are 11 Ph.D. physicists for whom this experiment will be the major research commitment. We will have 5.5 FTE Ph.D.'s, 2 FTE technicians, at at least 2 FTE graduate students in residence at Fermilab during the installation and operation phases of the experiment.

The spectrometer will be oriented with its magnetic field vertical. This allows data to be taken concurrently with operation of the Chicago Cyclotron Magnet upstream, bending the beam toward the East. This assumes that at beam energies less than the maximum, the CCM field is scaled accordingly, as has been the practice of the E98 group [3]. The spectrometer will be placed so that the beam is centered in the spectrometer with the CCM on. If the CCM is off, the beam can also be centered using magnets in Enclosure 104.

In addition to data-taking, we require test running at lower muon beam energy for calibration of the magnetic field in the spectrometer. We also need test runs with a hadron beam at several energies for calibration of the calorimeter and measurement of hadron punch-through probabilities.

III. DISCUSSION OF EXPERIMENTAL OBJECTIVES AND TECHNIQUE

A. Search for heavy neutral muons predicted by gauge theories, and for new particles giving rise to a two-muon final state.

A discussion of the theoretical motivation for searching for $\overline{M}^{o}$'s and a close examination of their possible experimental properties are contained in the original proposal. Briefly, the $\overline{M}^{o}$'s could be produced by deep-inelastic interactions of μ^{+}'s with nucleons via W^{+} exchange, and would quickly decay to $\mu^{+}\mu^{-}\bar{\nu}_{\mu}$ (B.R. $\approx$ 25%). The signature is one muon in, two out. The discovery of weak neutral currents [4] increases confidence in the Weinberg-Salam model (which contains no $\overline{M}^{o}$). At the same time, it imparts greater urgency to experiments which can test other predictions of gauge theories. For example, theories (III) and (V) catalogued by Bjorken and Llewellyn Smith[5] include neutral currents, require no M^{+} coupled to neutrinos (in agreement with experiment [6]) and also predict the existence of $\overline{M}^{o}$'s.

The trigger for $\overline{M}^{o}$'s and other inelastic multimuon processes is conceptually the same as that originally described. A coincidence is formed between a hadron shower signal from calorimeter counters upstream, and evidence of two muons in hodoscopes downstream of the shower. A quantitative description of the trigger and background rejection appears in Appendix 4. The trigger rate, dominated by inelastic scattering at low Q^{2} of one

muon in coincidence with an unvetoed muon in the same RF bucket, is less than 2×10^{-6} (per incident muon) at 10 MHz instantaneous rate.

The number of triggered and analyzed $\bar{M}^{o}$'s, using the same cross-section and branching ratio assumptions as on p. 19 of the original proposal, is:

M^o mass	Events/10^{12} muons
2 GeV/c^2	466
4	445
10	121

To suppress background from $\pi^- \to \mu^- \bar{\nu}_\mu$ decay, the original proposal described a set of kinematic cuts which removed about 1/2 of the signal as well. We expect that the higher density of information in the current version of the spectrometer will make such severe cuts unncessary. For example, the better calorimeter will allow us to reconstruct and cut on the missing (neutrino) energy.

It is important to emphasize the general nature of the particle search we will conduct. Apparent muon nonconservation can result from the weak decay of any new particle whose stronger decays are suppressed by old or new selection rules. Accordingly the capabilities of this experiment are restated in more general terms. With 225 GeV muons incident on Fe, the integrated luminosity is 3×10^{39} cm^{-2}. For example, this corresponds to 10^8 deep-inelastic muon interactions with $\nu > 50$ and $Q^2 > 2$. Compared to ordinary hadron reactions, each of these interactions is unusually violent, representing a prime source of new particle production. The excellent acceptance and trigger efficiency of the proposed spectrometer make it possible to detect most of the subset of these 10^8 interactions which contain one or more "directly produced" muons with energy $\gtrsim$ 20 GeV, in addition to the scattered muon. These are identified with high efficiency and reconstructed with negligible kinematic bias. The principal backgrounds are (1) $\pi \to \mu\nu$ decay, occurring at the 10^{-4} level,

and (2) inelastic μ tridents with one muon undetected. The identification and subtraction of these backgrounds is discussed in detail in the original proposal.

B. Measurement of Deep-Inelastic Virtual Compton Scattering

Since we discussed this measurement in Addendum I, new results from the U.C. Santa Barbara [7] and Rochester [8] groups have confirmed the anomaly originally observed at Cornell[9]: Inelastic processes involving two hadronic photons occur at rates typically one order of magnitude in excess of the parton-model predictions. Almost no related information exists in the much larger kinematic range accessible to this experiment at the Fermilab.

The trigger for Compton scattering is the same as for the $\overline{M}^{O}$ search. Evolution of the spectrometer design (part II) produces rate estimates approximately 70% of those in Addendum I, with considerably improved information on the final state.

Again, we emphasize that the virtual Compton scattering process [γ_v (spacelike) N → γ_v (timelike) X ; γ_v (timelike) → $\mu^+\mu^-$] is just one member of a general class of possible mechanisms for inelastic production of dimuons. For example, the timelike photon may be replaced by conventional or unconventional vector mesons. Detection of diffractive rather than deep-inelastic virtual photoproduction of massive dimuon states is discussed in some detail in a separate section (part D).

C. Deep Inelastic Muon Scattering

The spectrometer is well suited to a study of deep inelastic muon scattering, especially the behavior of the structure function νW_2 as a function of Q^2 and ν in the region $Q^2 > 150$ $(GeV/c)^2$.

The trigger has been designed to favor the high-Q^2 region by requiring an appreciable scattering displacement in the non-

bending (vertical) direction. Referring to Figs. 1 and 3, the trigger will require one or more counts from each of any two successive hodoscope banks, with no count in either of the associated beam-veto counters. In order to avoid biases in detection efficiency dependent on hadron energy, the trigger does not require a detected hadronic shower. Monte Carlo simulations give a total rate for this trigger of 2.6×10^{-6} triggers/incident muon, of which more than 80% are from real events. We have made conservative estimates of the background rates; the calculations are described in Appendix 4. None of the backgrounds presents a problem.

The reconstructed events will be characterized by $\sigma(1/E')$ between 7 and 11%. Coulomb scattering contributes 100-150 MeV/c uncertainty to the transverse momentum in the nonbending plane. The expected yield of triggered and analyzed events vs. Q^2 for 10^{12} muons at 225 GeV is shown in the table below:

Q^2 $(GeV/c)^2$	Events above this Q^2	Q^2 $(GeV/c)^2$	Events above this Q^2
40	7.8×10^5	160	8.2×10^3
60	3.6×10^5	180	3.3×10^3
80	1.7×10^5	200	1.3×10^3
100	8.8×10^4	220	450
120	4.1×10^4	240	152
140	1.9×10^4	260	48

D. Exploration of The Properties of ψ, ψ', and Other Massive Dimuon States

A quantitative calculation of ψ yields has been carried out. For conservatism, only transverse virtual photons having the usual ρ muoproduction flux and diffractive scattering from Fe were considered. Exact kinematics were used for Q^2_{min}, t_{min}, and t_{max} effects, with all masses finite. The E87 dimuon cross-section of .24 nb/Be nucleus at $Q^2 = 0$, $\nu = 150$ was used for all ν[11],

together with t_{min} restrictions on phase space. The cross-section and t slope parameter for Fe were scaled by $A^{2/3}$ from the Be values [10]. A ψ propagator = $1/(1 + Q^2/m_\psi^2)^2$ was used. For 225 GeV muons incident, the following cross-sections were obtained for ψ-like dimuon states. In each case we assume the same form for the propagator and the same value for the photon coupling constant.

Mass	$\sigma\mu\mu$ per Nucleon	Assumed $\mu\mu$ B. R. Relative to ψ	Effective $\sigma\mu\mu$ per Nucleon	$\mu\mu$ Decays in Target	
				Total	with 3 μ's penetrating 7 modules
(ψ) 3.1	11 pb.	1	11 pb	3×10^4	2×10^4
(ψ') 3.7	4	0.1	.4	1×10^3	700
6	.2	0.1	.02	50	35
9	.005	0.1	5×10^{-4}	1.3	1

The Q^2 - ν distribution of ψ's is shown in Fig. 6. The total number of $\psi \to \mu\mu$ decays occurring in the spectrometer target is 3×10^4, with $\sim$100 having $Q^2 > 10$.

Because of t_{min} effects, the calculated cross-sections are lower than one might naively expect. Even with the exceptionally high luminosity and acceptance in the proposed spectrometer, this method of search for higher mass ψ-like objects is limited. Higher energy muons would of course help, but e^+e^- rings (also of higher energies) would seem to be the best way of studying higher mass states.

Figure 6 illustrates two unique capabilities of this ψ experiment. The large sample ($2 - 3 \times 10^4$) of collected events permit a definitive (1%) measurement of g_A/g_V in $\psi\mu\mu$ coupling, if the beam helicity can be alternated. Unfortunately, this is a future development. Of immediate interest is the ψ production

rate at high $|q^2|$: a bin with median $q^2 = -m_\psi^2$ has $\approx$ 300 events. The q^2-dependence of the $\psi\mu\mu$ coupling (presumably ψ-γ coupling) therefore is measurable for $-15 < q^2 < 0$ as well as for $q^2 = 0$ (E87) and $q^2 = 9.6$ (SPEAR). A dramatic q^2-dependence of the type proposed in the "color" scheme of Bars and Peccei [12] would be easily detected.

A trigger for diffractive ψ production should not require the scattered muon either to be soft or to emerge at small angles. The former restriction removes most of the sample (cf. Fig. 6) and the latter deletes the high $-Q^2$ events. A promising trigger concept designed to suppress μ trident background is described in Appendix 4. The calculations required to specify the trigger acceptance and rate are not yet complete.

The ψ dimuons will be detected with chamber acceptance averaging 64% and mass resolution ranging from 6% in the best case to 10% for topologies with "minimal" information. The chief analysis background is expected to be incoherent muon tridents at the same low level as in E 87.

IV. FUTURE PLANS

The detector proposed here is well suited to the study of additional new physics when parameters of the Fermilab muon beam are extended. The most obvious parameter is muon energy. Weak interaction effects generally increase with energy, and the gain is especially dramatic when kinematic thresholds are involved. The dependence of M^o production on M^o mass and muon energy is discussed in the original Proposal 203. The deep-inelastic scattering data also will benefit from higher energy. In the proposed run, for example, raising E_μ from 225 to 300 GeV would increase the number of events with $Q^2 > 260$ $(GeV/c)^2$ from 50 to 1000. For diffractive muoproduction of vector particles (e.g., ψ's) the gain with increasing energy is dramatic, especially for exploration of higher mass states. Both t_{min} and threshold effects contribute to the improvement.

Control of muon helicity is a development with equally attractive possibilities for new measurements, particularly in the study of weak neutral currents. The implications for the muon-nucleon scattering cross-sections have been studied by Berman and Primack [13], Derman [14] and Suzuki [15]. Both the charge and helicity asymmetries increase as Q^2 and are of the order of a few percent at $Q^2 = 100$ (GeV/c)^2. The spectrometer we have proposed is particularly well suited to these measurements because of its high luminosity and acceptance, and symmetric detection of μ^+ and μ^-.

Another interesting problem is the search for an axial vector coupling in the muoproduction of ψ's. Present experimental limits on an axial component of the $\psi\mu\mu$ coupling are very weak. From $e^+e^- \to \mu^+\mu^-$ asymmetry measurements, we know only that $(g_A/g_V)^2 < 0.1$. In a broad view, such an interaction may be characterized without making specific assumptions about the Q^2 dependence of propagators and form factors. We emphasize that for $g_A/g_V << 1$, the search for g_A is better carried out with helicity rather than charge asymmetry measurements, because the former vary linearly with g_A/g_V, while the latter vary quadratically. In a comparison of cross-sections with well defined muon helicities at the presently proposed luminosity, the limit that can be set is in the range $g_A/g_V \lesssim 10^{-2}$, corresponding to a limit on the muon charge asymmetry in ψ-decay at the level of 10^{-4}!

Improvements to the muon beam of the types considered above in part can be made by increasing the accelerator energy. Continued improvements to the muon beam and its parent hadron beam are also needed. In particular, we note that **1)** the momentum range of the muon beam channel and its intensity can be increased without significant cost by the use of iron-focusing elements. **2)** the range and selectivity of the parent hadron beam should also be improved to increase the muon intensity at high momentum and to provide for the control of muon helicity.

Members of this group will continue their participation in the development of reasonable plans for effecting these essential improvements.

REFERENCES

1. J. J. Aubert et al., Phys. Rev. Lett. 33, 1404 (1974)
   J. E. Augustin et al., Phys. Rev. Lett. 33, 1406 (1974)
   C. Bacci et al., Phys. Rev. Lett. 33, 1408 (1974)
   G. Abrams et al., Phys. Rev. Lett. 33 1453 (1974).

2. J. P. Boymond et al., Phys. Rev. Lett. 33, 112 (1974)
   A. Benvenuti et al., Harvard, Pennsylvania, Wisconsin, Fermilab Preprint to be published.

3. T. B. W. Kirk, private communication.

4. F. J. Hasert et al., Phys. Lett. 46B, 138 (1973).

5. J. D. Bjorken and C. H. Llewellyn Smith, Phys. Rev. D7, 887 (1973).

6. B. C. Barish et al., Phys. Rev. Lett. 32, 1387 (1974).

7. D. O. Caldwell et al., Phys. Rev. Lett. 33, 868 (1974).

8. A. Melissinos, private communication.

9. J. F. Davis et al., Phys. Rev. Lett. 29, 1356 (1972)

10. The Fe (form factor)^2 was taken to be exp(-135 t).

11. NOTE ADDED IN PROOF: We have recently learned that the E 87 photoproduction cross-section is 16 nb, rather than 24 nb. All of our rates for Ψ production should be revised downward accordingly.

12. I. Bars and R. D. Peccei, "The Colorful ψ's", Stanford University Theoretical Reprint ITP-480, December, 1974.

13. S. M. Berman and J. R. Primack, "Weak Neutral Currents in Electron and Muon Scattering," SLAC Preprint, SLAC-PUB-1360 (TIE), December, 1973.

14. E. Derman, Phys. Rev. D7, 2755 (1973).

15. M. Suzuki, Nuc. Phys. B70, 154 (1974).

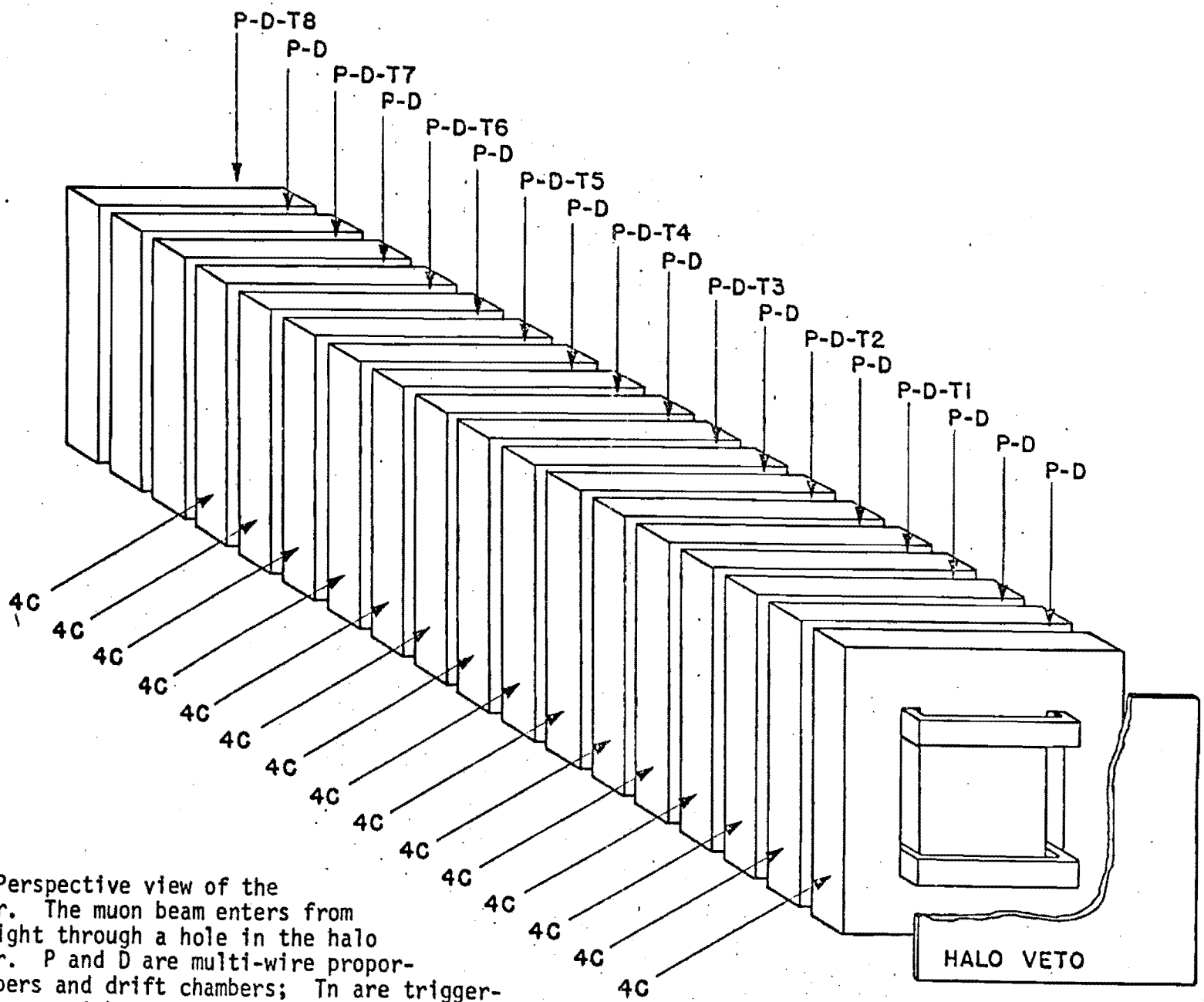

FIGURE 1. Perspective view of the spectrometer. The muon beam enters from the lower-right through a hole in the halo veto counter. P and D are multi-wire proportional chambers and drift chambers; Tn are trigger-hodoscope arrays with a beam veto/calorimeter counter. 4C indicates the four calorimeter counters within each magnet module. Also see Fig. 2 - 4.

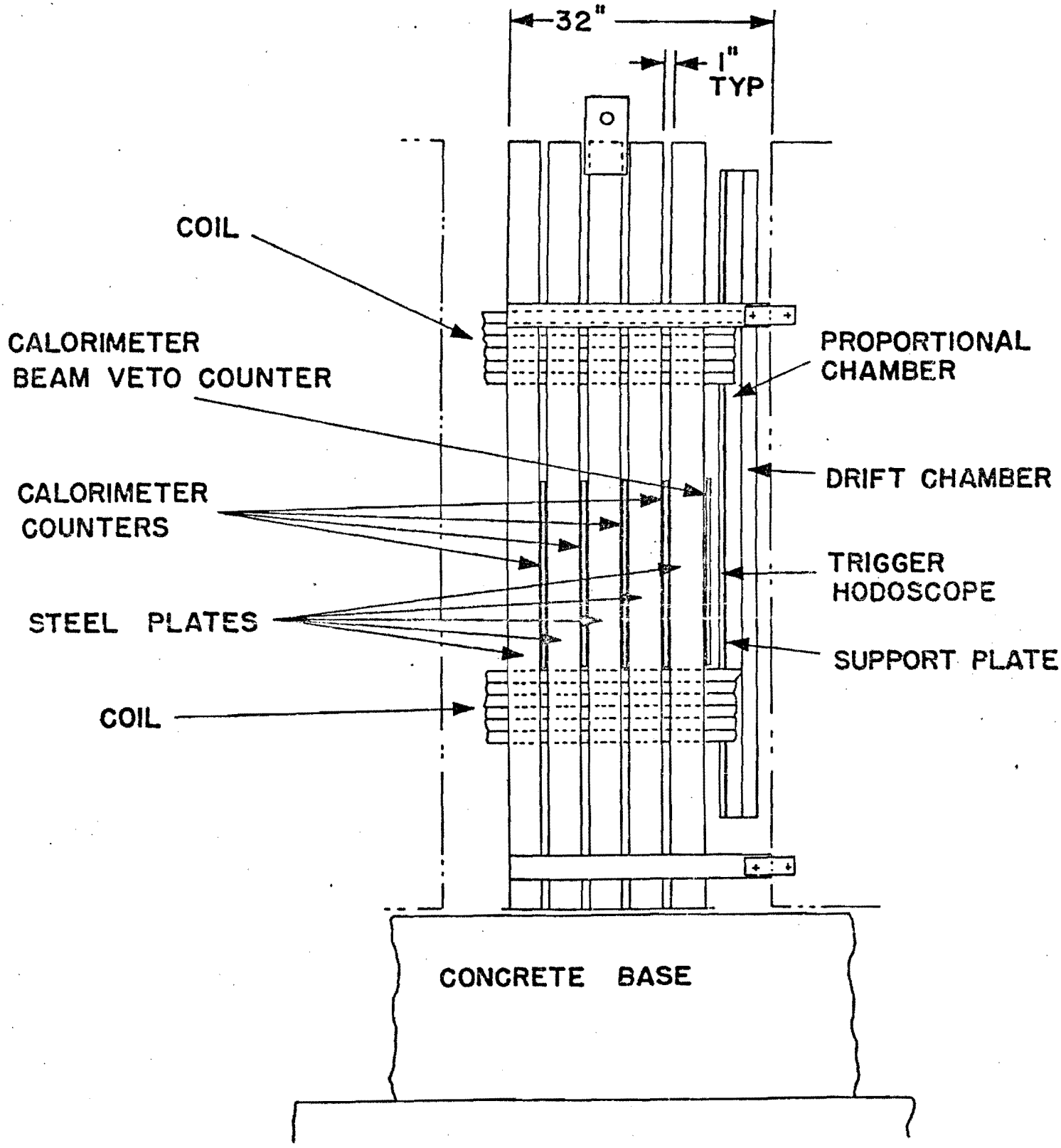

FIGURE 2. Elevation view showing detail of one module. The spectrometer consists of 18 of these modules.

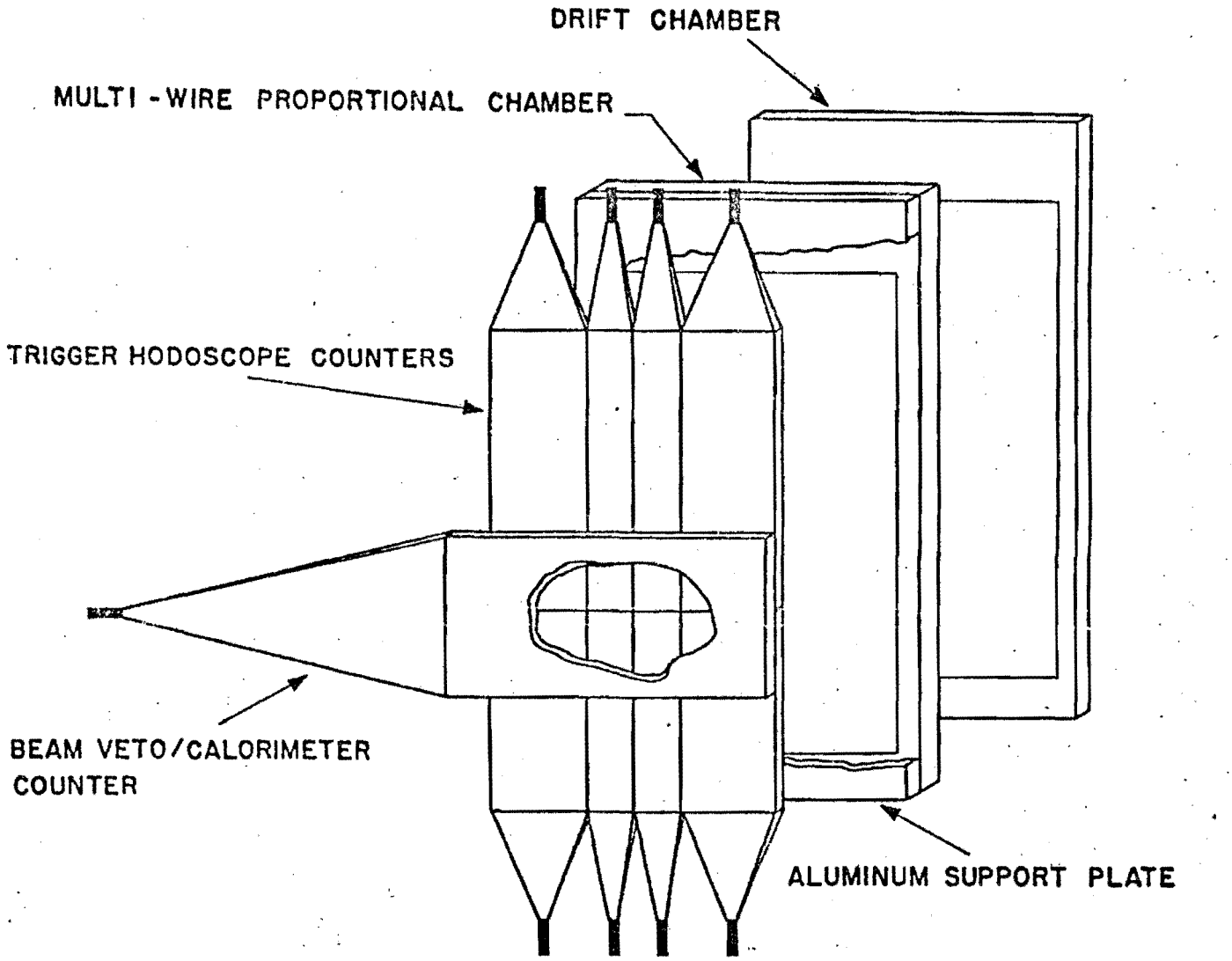

FIGURE 3. Exploded view of one trigger-detector assembly. All components are mounted on a single support plate to maintain alignment.

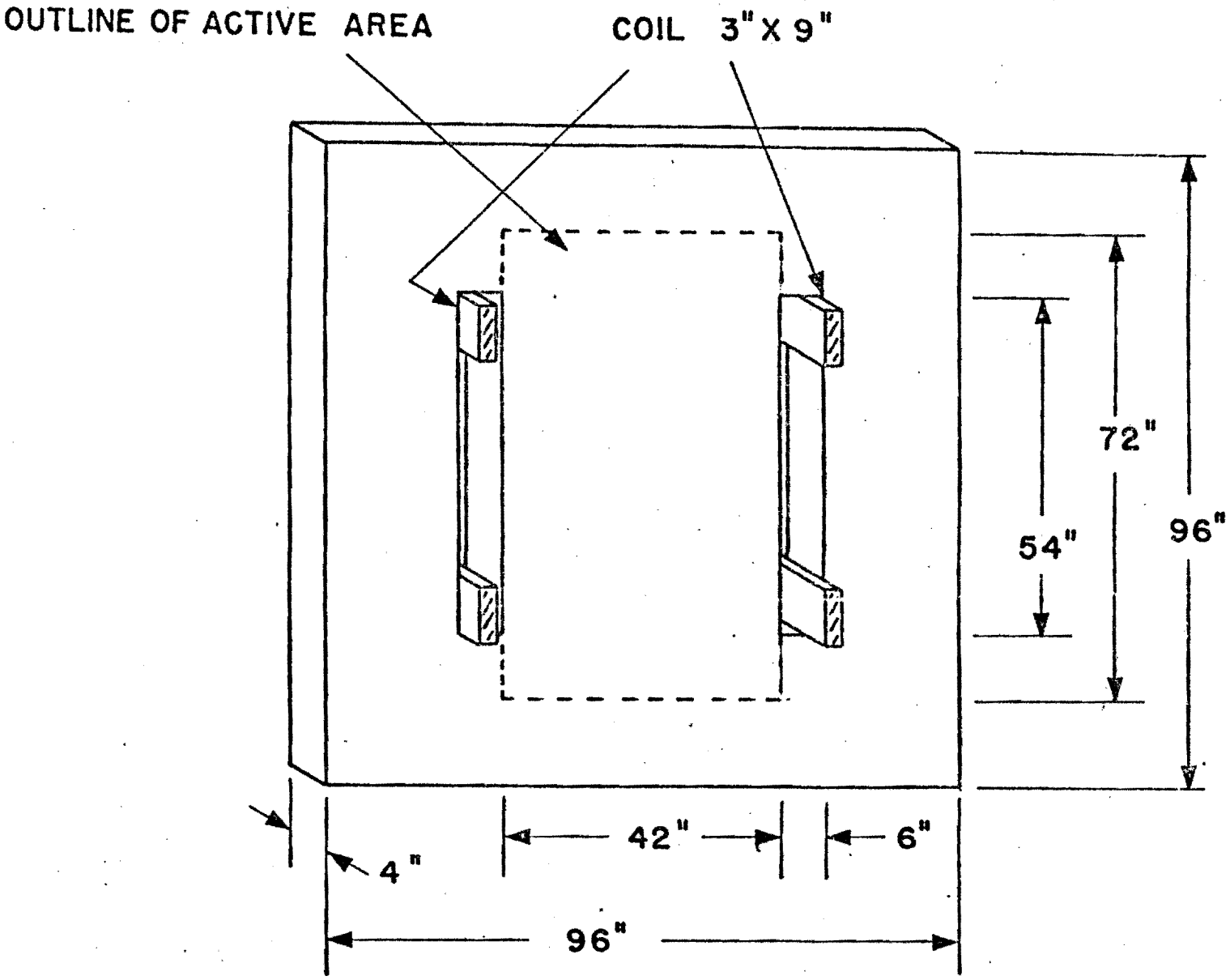

FIGURE 4. Magnet plate, detail.

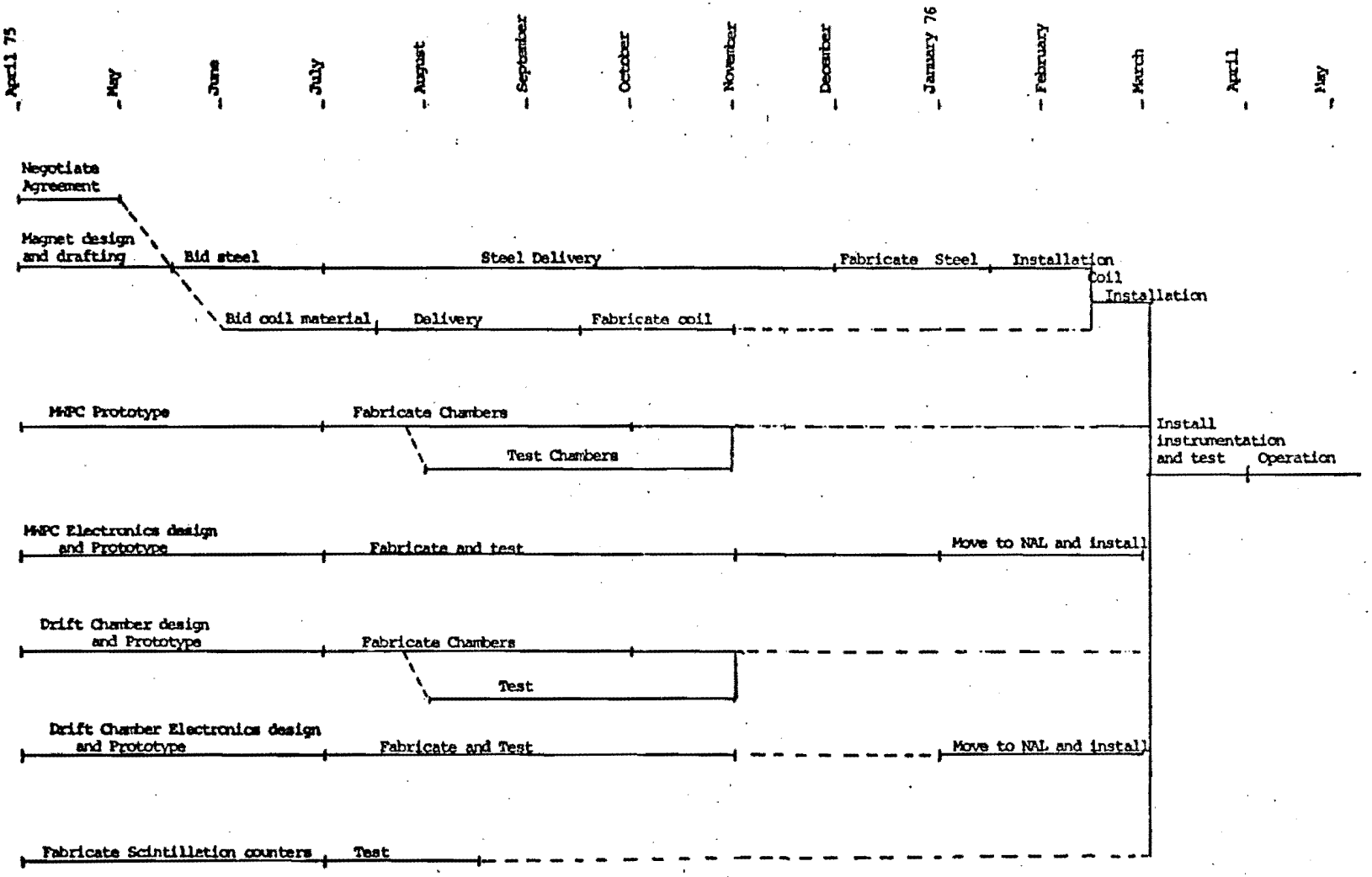

FIGURE 5. Design and fabrication schedule.

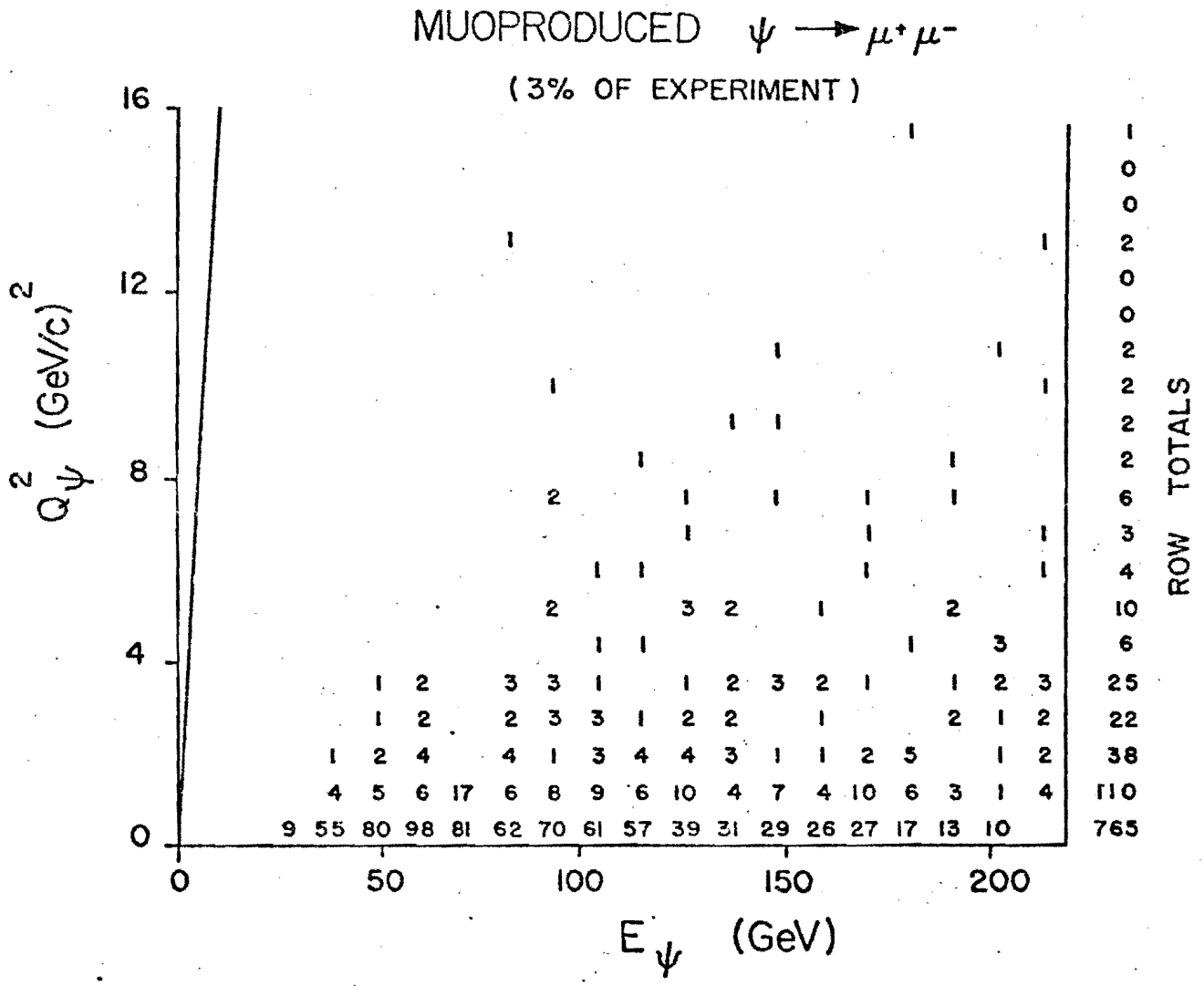

FIGURE 6: The Q^2 - ν ($\nu \approx E_\psi$) distribution of muoproduced ψ particles. The assumptions used in the Monte Carlo calculation are described in the text.

APPENDIX 1: MAGNET COST ESTIMATES

LAWRENCE RADIATION LABORATORY — UNIVERSITY OF CALIFORNIA

ENGINEERING NOTE

CODE	SERIAL	PAGE
AA0103	M4782 C	1 of 3

AUTHOR	DEPARTMENT	LOCATION	DATE
J. Gunn	Mechanical Engineering	Berkeley	December 2, 1974

PROGRAM — PROJECT — JOB

MECHANICAL ENGINEERING

COSTS, TIME STUDIES, ESTIMATING

TITLE

SECOND PARTIAL COST ESTIMATE FOR NAL EXP. P203

"A" Rev. 12/3/74 - DFR
"B" Rev. 2/7/75 - DFR
"C" Rev. 2/14/75 - DFR

This cost estimate covers only the iron-target iron magnet assembly, as discussed with A. R. Clark on January 28, 1975 for NAL Experiment P203. First proposal is on EN M4782. See UCLBL Dwg. 17L1934 for magnet module.

MAGNET STEEL PLATES - AISI 1020

Informal quote - Lukens Steel Company, Coatsville, Pennsylvania
17.8¢/lb, 5 month delivery (subject to escalation)
Estimated freight to Chicago: 2¢/lb

90 plates @ 10,633 lb/plate x 19.8¢/lb $189,480

MAGNET MODULE ASSEMBLY (18) COSTS

Labor to flame cut 180 holes (6" x 54" each) for coils and inserts: 367 hr @ $15/hr	5,505
Press insert into holes of each plate: 90 hr @ $15/hr	1,350
Weld up module: 244 hr @ $15/hr	3,660
Lifting beam for module assembly	500
Estimated freight Chicago to NAL @ 1¢/lb	9,569
	$ 20,584

ALUMINUM CONDUCTORS

Extruded alloy 1060F - 61% AICS conductivity
1.165 x 0.92 with 0.6 diam. hole x 60 ft straight section
Weight/ft = 0.954#
42 turns @ 120 ft/turn = 5,040 ft
Add 10% for spoilage = 480
5,520 ft (5,266 #)

Quote from New Jersey Aluminum Company, Elizabeth, N.J.

Tooling charge: $450		
Setup charge: 140	$	590
Plus $1.035/lb x 5,266 lb		5,450
Plus estimated shipping to NAL @ 3¢/lb		158
Conductor cost:	$	6,198

COIL FABRICATION

Aluminum hose barbs		
4/turn x 42 turns = 168 required @ $1.05 ea	$	176
Labor to weld to conductors		
C'bore: 56 hrs		
Weld: 56 hrs		
112 hrs @ $15/hr		1,680
Wrap conductors with heat shrinkable PVC tubing		
Material costs (9 rolls)		540
Installation 120 hr @ $15/hr		1,800
Thermal switches		
4 required @ $35 ea (installed)		140
Flow Switches		
1 required @ $200 ea (installed)		200
Hoses - 84 required @ 1.5 ft long @ 50¢/ft		63
Plus 84 hose clamps @ 75¢ ea		63
Plus installation: 32 hr @ $15/hr		480
Large supply hoses: 80 ft @ $2/ft		160
Manifolds - 2 required		
Materials		100
Labor: 30 hr @ $15/hr		450
Coil fabrication cost:	$	5,852

MAGNET ASSEMBLY COSTS

Stack steel module:	100 man-hours	
Install coil:	80 "	
Pressure and flow check	20 "	
200 man-hours @ $15/hr	$	3,000
Material		
1 x 2-1/2 x 80 ft stl bar = 0.25 x 680 ft		170
3/8 x 3 stl bar		204
Magnet assembly cost	$	3,374

NON MAGNETIC ABSORBER COSTS

Cast with wedged sides so as to fit into steel plates (90 plates)

11,332 # cast @ 80¢/lb $ 8,985

ENGINEERING DESIGN AND DRAFTING

160 hr @ $20/hr $ 3,200

SUPPORT (BASE) FOR MAGNET

Pour two concrete piers, 56 ft long $ 2,500

TOTAL	$240,173
Contingency 15%	36,026
GRAND TOTAL	$276,199

Inflation should be provided for at about 1% per month, for the appropriate time.

JG/DR:mp

APPENDIX 2 - INSTRUMENTATION COST ESTIMATE

Note: These cost estimates do not include institutional overhead costs. These have not been included because the method of calculation for overhead varies markedly from one institution to another making comparison difficult. Currently, 37% overhead is applied to materials and salary at LBL and 88% overhead is applied only to salary at Princeton. The estimates include shop labor charges for fabrication, assembly, and checkout wherever appropriate.

Calorimeter Counters (75 total)

Material	
Scintillator	on hand at LBL
Photomultipliers & bases	on hand at LBL
Light pipes, Al foil, etc.	$1425
Labor	$4135
TOTAL	$5560

Trigger Counters (64 total)

Material	
Scintillator	on hand at LBL
Photomultipliers & bases	on hand at LBL
Light pipes, Al foil , etc.	$ 512
Labor	$4557
TOTAL	$5069

Multiwire Proportional Chambers (20 total - 3 planes each)

Material (Al plate, G10, Wire, etc)	$22,521
Labor	
Electrical Shop	$ 7,276
Mechanical Shop	$ 7,741
Carpenter Shop	$ 565
TOTAL	$38,103

Drift Chambers (20 total - 1 plane each)	
Material (G10, wire, etc.)	$ 12,560
Labor (estimate)	20,000
TOTAL	$ 32,560
MWPC Electronics (4096 channels on hand; 8864 channels (+10% spares) to be constructed)	
Sense planes	
4096 channels	on hand at LBL
Additional 1952 channels + 10% spares @ 7.65	$ 16,426
Delay cable for above	on hand at Princeton (on loan to Fermilab Exp. 26)
Induced Planes	
6912 channels +10% spares @ 8.75	$ 66,528
TOTAL	$ 82,954
Drift Chamber Electronics	
320 channels @ $100	$ 32,000
Beam Telescope Counters and MWPC System	(partially on hand at Princeton) $ 2,000
Fast PDP-15 Camac Interface (estimate)	$ 5,000
Engineering and Drafting for Magnet Design	$ 3,200
GRAND TOTAL	$206,446

APPENDIX 3 - RESPONSIBILITIES AND PERSONNEL

I. Responsibilities for Design and Construction of the Spectrometer

A. Magnet

The cost of construction and installation of the magnet will be borne by the Fermilab. The engineering design, preparation of working drawings and supervision of fabrication and installation will be the responsibility of the experimenters. The design and drafting will be done at LBL, and the supervision of construction and installation will be performed by the Princeton and Fermilab contingents.

B. Instrumentation

The design and construction of the MWPC system, calorimeter, and trigger counters will be the responsibility of the LBL group. The drift chamber system, halo veto and beam telescope counters and small MWPC's will be the responsibility of the Princeton group. Interfacing the existing muon beam proportional chambers upstream of the muon lab (part of the muon scattering facility) to our system will be the responsibility of our Fermilab collaborator.

Standard fast-logic modules, photomultiplier power supplies, CAMAC crates, etc., will be supplied by PREP. For on-line use, a PDP-15 computer (48K core, 2 tapes) now at Princeton will probably be available. We are also considering the use of a standard BISON PDP-11 computer supplied by Fermilab.

II. RESPONSIBILITIES FOR OPERATION

The usual incidental supplies and expense (e.g., MWPC gas, travel, maintenance, etc.) will be the joint responsibility of the experimental groups. During installation, testing, and data collection the groups will maintain the following full-time equivalent manpower in residence at the Fermilab:

From LBL	3.5	FTE Ph.D. Physicits
	2.0	FTE Technicians
	$\geq$ 2.0	FTE Graduate Ph.D. Thesis Students
From Princeton	1.5	FTE Ph.D. Physicits
	0 or 1	FTE Graduate Ph.D. Thesis Student
From Fermilab	.5	FTE Ph.D. Physicists
TOTALS	5.5	FTE Ph.D. Physicists
	2.0	FTE Technicians
	2 - 3	Graduate Students

III. RESPONSIBILITIES FOR DATA ANALYSIS

Analysis of the data will be the joint responsibility of the experimenters. Preliminary tape compression will be performed on the Princeton PDP15 when it is not in on-line service. A large part of the event reconstruction will be done by the LBL 7600. Analysis of summary data will be performed at each institution.

IV. COMMITMENTS TO OTHER EXPERIMENTS BY PARTICIPANTS IN THIS PROPOSAL

LBL

A.R. Clark	Bevalac Exp. 209H (Complete CY75)
E.S. Groves	ISR (Letter of intent for experiment in FY77)
L.T. Kerth	Bevalac Exp. 209H (Complete CY75)
S.C. Loken	Fermilab Exp. 26 (Complete mid-year CY75)
M. Strovink	Fermilab Exp. 26 (Complete mid-year CY75)
W. Wenzel	ISR (Letter of intent for experiment in FY77)

PRINCETON

R. Cester	BNL Exp. 661 (CY75)
	Fermilab Exp. 302*
	BNL Exp. 646 (CY77)
F.C. Shoemaker	No other research commitments
M.S. Witherell	BNL Exp. 661 (CY75)
	Fermilab Exp. 302*
P. Surko	No other research commitments

FERMILAB

R.P. Johnson	Fermilab Exp. (Complete CY75)

*Fermilab E302 has first priority on the research activities of R. Cester and M.S. Witherell. If construction of the E302 $\bar{p}$ beam occurs on a schedule which results in an overlap between installation of E302 and operation of this experiment, the Princeton group intends to maintain its strength by bringing other scientific personnel into the experiment.

V. COMMUNICATION WITH THE FERMILAB

At present, the spokesman for the experiment is M. Strovink. During the construction phase of the experiment, the spokesman will be L.T. Kerth. During installation and operation of the experiment, communication with the laboratory will be the responsibility of one or more of the experimenters who are in residence at the Fermilab.

APPENDIX 4 - TRIGGER LOGIC AND BEAM REOUIREMENTS

A. General Considerations

Figures 1-3 indicate the calorimeter counters and hodoscopes which will be used for all trigger logic. We shall describe how the counter system can be used to study the various processes discussed in the proposal. Features which are common to all these conditions, the muon beam and associated muon halo, will be considered here.

1) Muon Beam:

The beam logic requires that the incident muon pass through the last bend in the muon beam (enclosure 104) without hitting the magnets. A beam hodoscope at 104 allows determination of muon angle. A fine grained hodoscope (10 x 10 counters) at the front of the spectrometer completes this angle measurement. In addition, requiring one and only one count in the hodoscope will eliminate all but 2% of the R.F. buckets containing two beam muons (see discussion of two muon trigger). To suppress further the background trigger rate from two muons in the same R.F. bucket, a third beam hodoscope at the downstream end of the spectrometer measures deflection perpendicular to the bend plane of the magnet. This is used to veto beam muons which are not scattered by more than multiple Coulomb scattering in the magnet. These two measures result in a suppression of 10^{-3} or better for two simultaneous beam muons.

2) Halo Veto:

A large counter array in front of the spectrometer (see Figure 1) is used to veto possible triggers from accidental beam halo coincidences. In order to construct a highly efficient counter with good time resolution we use the knowledge about the spatial distribution of halo muons gained from previous muon running. By using small counters close to the muon beam with larger ones outside (with less stringent requirements), we expect to obtain a halo suppression of 10^{-4}.

B. Two Muon Trigger

The trigger for M^o events uses calorimeter counters C1-C75 and trigger hodoscopes T1-T8. A trigger signifying a hadron interaction will use the fact that a typical hadron shower is spread through at least one entire module (5 iron slabs and counters) whereas an electromagnetic shower loses essentially all its energy in one slab (6 rl). A multi-muon final state requires two or more separate counts in a given bank of trigger hodoscopes. A coincidence from three sequential hodoscopes, separated by a total of 60 radiation lengths, is used to suppress trigger background from multiple showers. To suppress triggers from penetrating hadronic showers, the vertex location from the calorimeter counters is used to deaden hodoscopes immediately downstream of the vertex. On average, 3200 g/cm^2 of iron protect the hodoscope coincidence from remnants of the upstream shower. A Monte Carlo simulation of this trigger system yields a detection efficiency which varies from 45% at a M^o mass of 2 GeV/c^2 to 56% for M^o's of 10 GeV/c^2.

Background Triggers:

The most serious source of background triggers is associated with two beam muons in the same RF bucket. One of the muons interacts giving the required hadronic shower and the two muons are detected downstream. This rate is easily estimated.

Probability of two muons in the same RF bucket (at 10 MHz)	0.2
Probability of not vetoing two muon bucket (see previous discussion.)	$<10^{-3}$
Interaction probability (deep inelastic scattering with $\nu > 15$ GeV)	1.2×10^{-2}
Trigger Rate	2.4×10^{-6}

Triggers from the remnants of hadronic showers are eliminated by requiring a separation of seven modules (12 ft of iron) between the vertex and the last hodoscope in the coincidence. The rate can be estimated:

Probability of interaction with $\nu > 25$ GeV	6.5×10^{-3}
Probability of 12 ft penetration*	10^{-4}
Trigger Rate	6.5×10^{-7}

A third background trigger comes from multiple showers. The requirement that three hodoscopes in sequence detect more than one particle will eliminate this problem since the banks are separated by a total of 60 RL. For the case of multiple electromagnetic showers we get

Probability of interaction $\nu > 15$ GeV	1.2×10^{-2}
Probability of three independent electromagnetic showers	$(3 \times 10^{-2})^3$
Trigger Rate	3×10^{-7}

For the case of two hadron interactions, one of which penetrates four modules and triggers the hodoscopes the rate is lower.

Interaction Probability $\nu > 15$ GeV	1.2×10^{-2}
Probability of a hadron shower penetrating four modules	10^{-5}
Trigger Rate	1.2×10^{-7}

RF buckets which have a halo muon and a beam muon will be vetoed (see previous discussion). Any inefficiency in this veto will cause accidental triggers.

Probability of interaction $\nu > 15$ GeV	1.2×10^{-2}
Probability of halo in the same RF bucket	$< .2$
Veto inefficiency	10^{-4}
Trigger Rate	2.4×10^{-7}

* O. Fackler (private communication)

C. Deep Inelastic Muon Scattering Trigger

Real Rate

The trigger rate for real events from inelastic muon scattering is based on a Monte Carlo calculation with the following assumptions:

Beam: E_o = 225 GeV; size - 6" high x 8" wide; beam is incident on the face of the spectrometer centered horizontally and 6" below the median plane.

Cross Section: νW_2 is taken from a parameterization of the SLAC data.

Spectrometer: As described in Section II above.

Trigger: Scattered mu is required to pass through two successive trigger banks outside of the beam-veto region.

The beam muon and the scattered muon have been propagated through the iron by the simulation program, including the effects of single- and multiple-Coulomb scattering, μ-e scattering and muon bremsstrahlung.

Rate for real triggers 2.2×10^{-6}

Background Rates:

The most important backgrounds come from two step processes where the incident muon suffers a large energy loss and is deflected out of the spectrometer without triggering, and a scattered muon is faked by either an accidental halo muon or by long range "punch-through" from a hadronic shower.

We have made conservative estimates of these various trigger rates. Muon losses from μ-e scattering, bremsstrahlung, and low Q^2, high-ν inelastic scattering were studied with Monte Carlo programs. Data on punch-through was obtained from Fermilab experiment E-104*; an instantaneous beam rate of 10^7/sec and a halo veto inefficiency of 10^{-4} were assumed. The resulting rates are shown below:

* O. Fackler (private communication)

a) Beam loss rate from coulomb and μ-e scattering and muon bremmsstrahlung 5.5×10^{-4}

Probability of halo accidental 0.2

Halo veto inefficiency 10^{-4}

Total Rate 0.11×10^{-7}

b) Rate for low-Q^2 high ν inelastic scatter with scattered muon lost from beam veto; the scattered muon signature is completed by hadron punch through. This is calculated by folding together the depth-dependent muon loss rate and the probability of punch-through beyond that point. The minimum punch-through rate used was 2×10^{-3}.

Total Rate 0.4×10^{-6}

c) Same as b) except that the trigger is completed by a halo accidental.

Rate for loss of scattered muon from beam veto 1.1×10^{-4}

Probability of halo accidental 0.2

Halo veto inefficiency 10^{-4}

Total Rate 0.02×10^{-7}

Total rate - real + background 2.61×10^{-6}

D. Three Muon Trigger

Three-muon final states not associated with a hadron shower at the interaction vetex do not satisfy the multimuon-shower trigger described in (B) above. For this case a shower-independent trigger will be used, which requires at least three counts in each of three successive trigger hodoscopes. Background triggers from hadron showers [see (B)] are suppressed by requiring at least two of the banks to have exactly three counts. With this requirement, accidental counts from soft electromagnetic showers in the iron upstream of each counter will create a negligible inefficiency.

More serious trigger background is caused by muon tridents which have large (~1 μb/nucleus) production cross section. The most common tridents have small pair energy and opening angle. These are suppressed by requiring one of the three counts in each hodoscope to be separated from the beam area by ≈6" in the vertical

(nonbending) plane. The soft pair muons are bent out of the spectrometer active area before their vertical Coulomb scattering displacement exceeds ≈2". Fortunately, the mean vertical displacement at the exit from the active area varies only with the fourth root of the muon energy. The detailed muon-trident simulations which will set the limit on this background trigger rate are not yet complete.